Zeeman effect

Max-Planck-Institut für Kernphysik,
Saupfercheckweg 1, Heidelberg

22nd May 2006

Introduction

The most important experimental technique triggering the development of the modern atomic theory is spectroscopy, the observation of the characteristic wavelengths of light that atoms can absorb and emit. A so-called wavelength dispersive element such as a waterdrop, a prism or a grating, spatially separates different wavelengths of light emitted from one source. If the light source emits white light, a band of all colours will be found after the light passes the wavelength dispersive element (*e.g.* rainbow). Observing the light from a lamp that contains only atoms of a certain element, one finds distinct lines instead of the complete band on the detector. The positioning of the lines on the detector is called a spectrum, and the corresponding wavelengths are hence called 'spectral lines' of the element.

The additional information needed to be able to draw conclusions about the atomic structure from spectral lines was provided by the experimental observation of Rutherford that in an atom, electrons surround a heavy, positively charged nucleus in the center, and by Planck's explanation of the blackbody spectrum by quanta of light, photons, whose energy E_{ph} is connected with the wavelength λ by

$$E_{ph} = h\nu = \frac{hc}{\lambda} \ , \tag{1}$$

where ν is the frequency, h is the Planck constant and c is the speed of light. With this knowledge it became clear that electrons in an atom can occupy only certain energy levels E_i, and that the transition of an electron from a higher energy level E_2 to a lower energy level E_1 leads to the emission of a photon: $E_2 - E_1 = E_{ph}$. The energy needed to lift the electron to the higher, 'excited' energy level can be provided by absorption of a photon of the very same energy or by collisions.

The increasing experimental precision reached with spectroscopy inspired scientists to propose different atomic models, leading to the development of quantum

mechanics. With refinements to the quantum mechanical description of the atom, relativistic quantum mechanics (necessary to explain the the splitting of energy levels of same main quantum number n) and quantum electrodynamics (QED, necessary to explain the splitting of levels with same quantum number j but different quantum number l), theory is by now able to make highly accurate predictions about the atomic structure.

Effects of an external magnetic field on the atomic structure

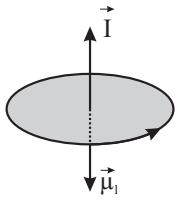

Figure 1: Classical model of an electron with angular momentum $\mathbf{l}$ inducing an angular magnetic moment $\vec{\mu}_l$

If the atom is placed in an external magnetic field, the atomic energy levels are split and the observed spectrum changes. This was first observed by the dutch physicist Pieter Zeeman and is hence called the Zeeman effect. In an intuitive approach to explain the Zeeman effect, consider an atom with an electron with charge e moving with the speed v around the nucleus on a Bohr orbit with radius r. This orbiting electron can be described by a current

$$I = -e \cdot \frac{v}{2\pi r} \tag{2}$$

inducing an orbital magnetic moment

$$\vec{\mu}_l = I \cdot \mathbf{A} = I \cdot \pi r^2 \mathbf{n} = \frac{evr}{2}\mathbf{n} \ , \tag{3}$$

where $\mathbf{A} = \pi r^2 \mathbf{n}$ is the area vector perpendicular to the orbit area πr^2. The angular momentum of the electron with mass m_e is

$$\mathbf{l} = \mathbf{r} \times \mathbf{p} = m_e \cdot r \cdot v \cdot \mathbf{n} \ . \tag{4}$$

An external magnetic field $\mathbf{B}$ interacts with the angular magnetic moment and, hence, changes the electron's potential energy:

$$\Delta E_{pot} = -\vec{\mu}_l \cdot \mathbf{B} = \frac{e}{2m_e} \cdot \mathbf{l} \cdot \mathbf{B} \tag{5}$$

Using the direction of the magnetic field vector $\mathbf{B}$ as quantisation axis z and the quantised angular momentum of the electron

$$|\mathbf{l}| = \sqrt{l(l+1)}\hbar \quad \text{with} \quad l = 0, 1, \ldots, n-1 \quad \text{and} \tag{6}$$

$$l_z = m_l \cdot \hbar \qquad \text{with} \quad -l \leq m_l \leq l \ , \tag{7}$$

equation (5) can be simplified to

$$\Delta E_{pot} = \frac{e \cdot \hbar}{2m_e} \cdot m_l \cdot B = \mu_B \cdot m_l \cdot B \ , \tag{8}$$

where μ_B is called the Bohr magneton. The energy shift of the electron's original energy level by ΔE_{pot} due to the coupling of the external magnetic field to the electron's angular magnetic moment leads to a splitting of the original level into the previously degenerated $2l + 1$ sublevels of same angular momentum l but different magnetic quantum number m_l.

The quantum mechanical way for deriving this energy splitting where also the electron spin is taken into account starts off by treating the external magnetic field as a perturbation $\hat{H}_B$ of the unperturbed Hamilton Operator $\hat{H}_0$. In general, an atom with more than one electron has to be considered. In the case of an external magnetic field that is small as compared to the magnetic coupling energies between the i electrons' orbital and spin momenta $\mathbf{l}_i$ and $\mathbf{s}_i$, respectively, one may use the so-called LS-coupling approximation. This approximation is appropriate when the coupling energy between the different electrons' orbital momenta is large as compared to the coupling of a single electron's orbital momentum with the same electron's spin momentum. Hence, all orbital and spin momenta are added seperately to total orbital and total spin momenta $\mathbf{L}$ and $\mathbf{S}$ before determining the total angular momentum $\mathbf{J}$:

$$\mathbf{L} = \sum_i \mathbf{l}_i \qquad \text{with} \qquad |\mathbf{L}| = \sqrt{L(L+1)}\hbar \ , \tag{9}$$

$$\mathbf{S} = \sum_i \mathbf{s}_i \qquad \text{with} \qquad |\mathbf{S}| = \sqrt{S(S+1)}\hbar \ , \tag{10}$$

$$\mathbf{J} = \mathbf{L} + \mathbf{S} \qquad \text{with} \qquad |\mathbf{J}| = \sqrt{J(J+1)}\hbar \ , \tag{11}$$

$$J_z = M_J \cdot \hbar \qquad \text{with} \qquad -J \leq M_J \leq J \ . \tag{12}$$

With these momenta introduced, the Hamiltonian of an atom in an external magnetic field is

$$\hat{H}_0 + \hat{H}_B = \hat{H}_0 - \frac{\mu_B}{\hbar} (\mathbf{J} + \mathbf{S}) \cdot \mathbf{B} \ , \tag{13}$$

and the solution for the shift of the level energy becomes

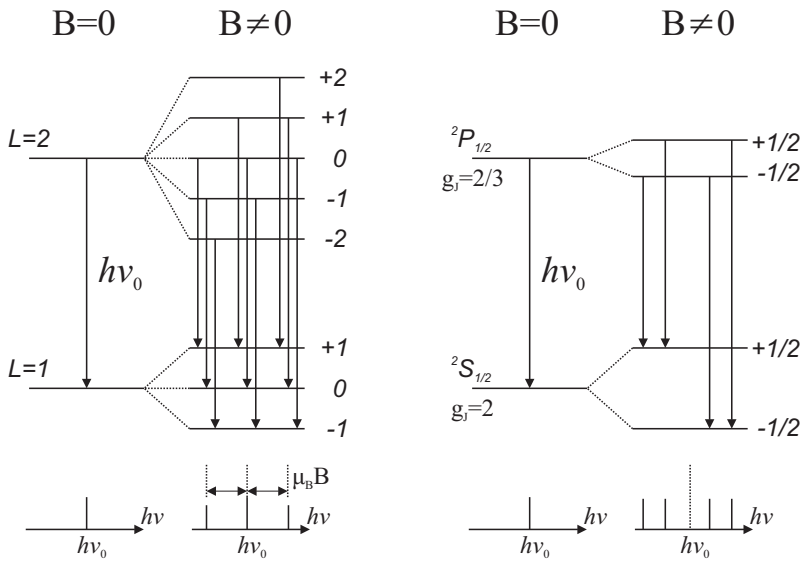

Figure 2: Left: Normal Zeeman effect for a d → p transition. The field splits the degenerate M_J levels by $\Delta E = \mu_B \cdot B \cdot M_J$. Right: Anomalous Zeeman effect. Here, the levels are split by $\Delta E = \mu_B \cdot B \cdot M_J \cdot g_J$. In both cases, transitions can occur if $\Delta m_J = 0,\pm 1$.

$$\Delta E_{pot} = \mu_B \cdot B \cdot M_J \cdot g_J \tag{14}$$

$$g_J = 1 + \frac{J(J+1) + S(S+1) - L(L+1)}{2J(J+1)} , \tag{15}$$

with the Landé factor g_J.

If all electron spins in the atom cancel each other, *i.e.* in the case of $S = 0$, $g_J = 1$ is obtained and equation (14) becomes identical to equation (5). For historical reasons, the splitting in absence of spin is called the *normal* Zeeman effect whereas, since the electron spin was not yet discovered and the observed features seen in the spectra were not understood, the more general case with $S \neq 0$ was named the *anomalous* Zeeman effect. In the normal Zeeman effect, the size of the energy splitting from the unperturbed level energy depends only on the magnetic quantum number m_l and is, hence, of the same size for all levels in the atom. In the case of the anomalous Zeeman effect, the energy splitting depends on the quantum numbers J, L and S, which is reflected by more complicated structures observed in the corresponding spectra (see Fig. 2).

In a strong external field, the LS-coupling approximation is no longer appropriate. The field-induced precessions are so rapid that one has to consider the total orbital momentum L and spin S as they individually precess about **B**, that is, the effect of **B** is effectively to decouple L from S, rendering J meaningless. This is called the Paschen-Back effect.

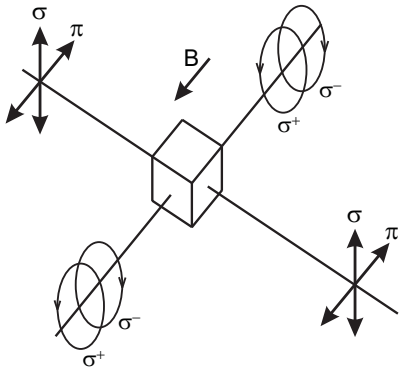

Figure 3: Isometric depiction of the polarisation of the different Zeeman components.

Selection rules and polarisation of emitted light

In transitions from an excited level i to a lower level k, a photon with the difference energy $E_{ph} = \Delta E = E_i - E_k$ is emitted. Still, as indicated in Fig. 2, not all energy differences between existing levels are actually found in the spectra. The reason is that not only the energy, but also momentum conservation, angular momentum conservation and symmetry rules play a role on whether or not a transition can occur. Only those transitions are allowed where the transition dipole matrix element

$$\mathbf{M}_{ik} = e \int \psi_i^* \; \mathbf{r} \; \psi_k \, dV \tag{16}$$

has at least one non-zero component

$$(M_{ik})_q = e \int \psi_i^* \; q \; \psi_k \, dq \quad , \text{with } q = x, y, z \; . \tag{17}$$

Evaluating these three integrals yields that only those transitions have non-zero components where the change of the magnetic quantum number fulfills $\Delta M_J = M_{J,i} - M_{J,k} = 0, \pm 1$. Furthermore, electric dipole transitions require that the change of the total orbital momentum be $\Delta L = L_i - L_k = \pm 1$ and that the spin does not change, *i.e.* $\Delta S = 0$.

If the quantisation axis (*i.e.* the direction of the magnetic field vector) is the z-axis, the matrix element component $(M_{ik})_z$ is the only non-zero one for $\Delta M_J = 0$ (so-called 'π'-) transitions. Considering a dipole and its characteristics of emission, this means the dipole is oscillating along the axis of the magnetic field vector and, hence, does not emit any radiation in that direction. Also, since the electric field vector is oscillating in only one direction, also the field vector of the emitted light wave oscillates in this direction, meaning that the light emitted by $\Delta M_J = 0$ transitions is linearly polarised (see Fig. 3).

In the case of $\Delta M_J = \pm 1$ ('σ'-) transitions, $(M_{ik})_z$ is zero and both $(M_{ik})_x$ and $(M_{ik})_y$ are non-zero and equal in magnitude, but phase-shifted by $\pi/2$. This phase shift between the two superimposed dipoles leads to the observation of circularly polarised light when viewing in z-direction ('longitudinally'). Viewing the emitted light in x- or y-direction ('transversal'), only the projection of the superimposed dipoles is seen, and thus the light from $\Delta M_J = \pm 1$ transitions appears linearly polarised when observed transversal to the magnetic field vector.

The experiment

The experiment consists of two parts. In the first part, you will observe the Zeeman effect in both transversal and longitudinal direction, and study the polarisation of the observed light. The second part of the experiment is dedicated to precision spectroscopy using a grating spectrometer.

In both parts of the experiment, you will study the light emitted from a cadmium (Cd) lamp. The electronic configuration of Cd is $[\mathrm{Kr}]4\mathrm{d}^{10}5\mathrm{s}^2$. In this configuration, all electronic spins compensate each other, such that $S = 0$. In the visible, the spectrum of Cd consists of four lines, as listed in table 1.

Table 1: Spectral lines of Cd in the visible

Color	violet	blue	green	red
Wavelength [nm]	467.9	480.1	508.7	643.8

All measurements will be performed using the the red line at $\lambda_0 = 643.8$ nm, ($\nu_0 = 465.7$ THz) emitted by the electronic transition between the two excited levels $^1\mathrm{D}_2 \rightarrow {}^1\mathrm{P}_1$ in the fifth shell of Cd.

Part I: Spectroscopy of the Zeeman effect

The expected shift of the emitted wavelengths due to the external magnetic field is well below 0.1 nm, hence a high resolution device has to be used in order to observe the effect. In this experiment, a Lummer-Gehrcke plate is used (see Fig. 4). The Lummer-Gehrcke plate is a quartz-glass plate with extremely plane parallel surfaces. Light is coupled into the plate by a prism and then reflected back and forth repeatedly inside of the plate close to the angle of total reflection. Thus, a small fraction of the light intensity emerges at each reflection point and travels at an angle of $\alpha \approx 90°$ to the surface normal. The emerging rays are observed with a telescope focused to infinity behind the Lummer-Gehrcke plate. Since the thickness of the

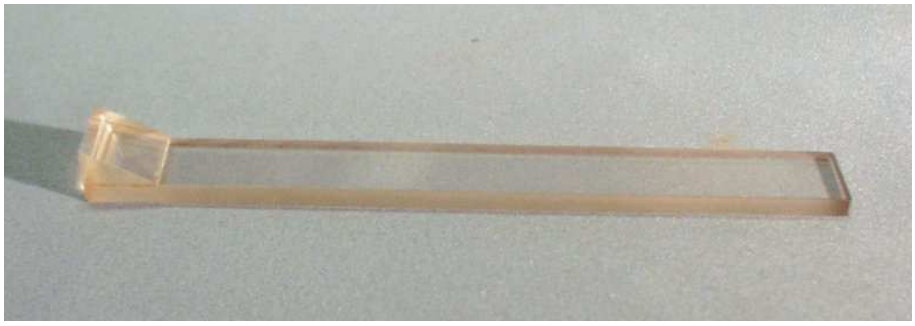

Figure 4: Lummer-Gehrcke-Interferometer.

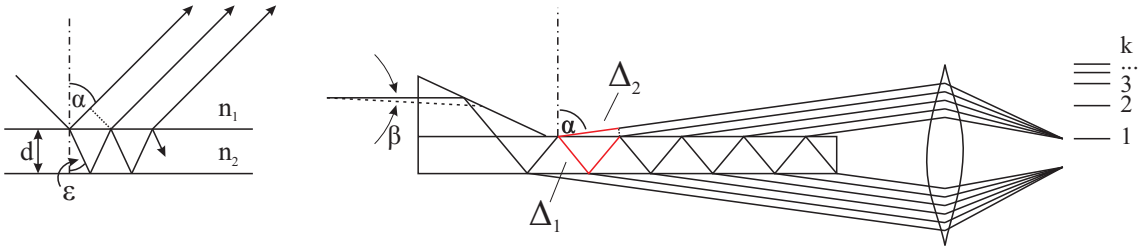

Figure 5: Left: Schematic to illustrate optical retardation using a glass plate. Right: Lummer-Gehrcke plate.

plate is much smaller than its length and because of the high reflection coefficient, many rays can interfere with each other, resulting in a very high resolution.

As shown in Fig. 5 (left side), the optical retardation between two light rays from a glass plate, where one was reflected inside the plate once, is given by

$$\Delta = 2n_2 \cdot \frac{d}{\cos\epsilon} - 2n_1 \cdot d \cdot \tan\epsilon \cdot \sin\alpha \ , \tag{18}$$

where d is the thickness of the plate, n_1 and n_2 are the refractive indices outside and inside the plate, and α and ϵ are the angles of the light to the surface normal outside and inside the plate, respectively. Using $\sin\alpha = \frac{n_2}{n_1}\sin\epsilon$ and $\sin^2\epsilon + \cos^2\epsilon = 1$, Eq. 18 becomes

$$\Delta = 2n_2 \cdot d \cdot \cos\epsilon = 2 \cdot d \cdot \sqrt{n_2^2 - n_1^2 \sin^2\alpha} \ . \tag{19}$$

In the case of the Lummer-Gehrcke plate, the light is coupled into the plate by a prism to allow angles $\alpha \approx 90°$ at the limit of total reflection. For a plate with $n_2 = n$ used in air ($n_1 \approx 1$) Eq. 19 reduces to

$$\Delta = \Delta_1 - \Delta_2 = 2d \cdot \sqrt{n^2 - 1} \ , \tag{20}$$

were Δ_i are indicated in the right part of Fig. 5. For constructive interference, the optical retardation has to fulfill $\Delta = m \cdot \lambda$, where k is an integer number and λ is

the wavelength of the interfering light. Obviously, whether or not constructive interference occurs when observing the Lummer-Gehrcke plate with a telescope depends on the wavelength λ and on the exiting angle α, which again depends on the angle β at which the light enters the Lummer-Gehrcke plate. For a given wavelength λ, one obtains many orders k for the different incoming angles β at which the emerging light beams interfere constructively (see Fig. 6).

One finds spatial overlap between the order k of wavelength $\lambda+\Delta\lambda$ and the order $(k+1)$ of wavelength λ if

$$k \cdot (\lambda + \Delta\lambda) = (k+1) \cdot \lambda \;\rightarrow\; \Delta\lambda = \frac{\lambda}{k} \; . \tag{21}$$

With Eq. 20 one finds the free spectral range of the Lummer-Gehrcke plate to be

$$\Delta\lambda = \frac{\lambda^2}{2d \cdot \sqrt{n^2-1}} \; . \tag{22}$$

In first approximation, a small change in wavelength $\delta\lambda < \Delta\lambda$ leads to a shift

$$\delta\lambda = \frac{\delta a}{\Delta a} \cdot \Delta\lambda \; , \tag{23}$$

where δa is the distance between the line with wavelength $\lambda+\delta\lambda$ from the position of the line with wavelength λ, and Δa is the distance of two orders k and $k+1$ of wavelength λ. Hence, for a small wavelength shift as it is induced *e.g.* by the Zeeman effect, one obtains

$$\delta\lambda = \frac{\delta a}{\Delta a} \cdot \frac{\lambda^2}{2d \cdot \sqrt{n^2-1}} \; . \tag{24}$$

The experimental setup is sketched in Fig. 7. The Cd lamp is placed between the pole shoes of a magnet. Light emitted from the lamp enters the Lummer-Gehrcke plate after passing a red filter (selecting the red spectral line). The magnet can be rotated by 90°, such that the lamp can be observed both in transversal direction to the magnetic field (as shown in Fig. 7) or, through a hole in the pole shoes, in longitudinal direction of the magnetic field. The interference pattern generated by the Lummer-Gehrcke plate is observed with a telescope. One can place a polarizer and a $\lambda/4$ plate between the Lummer-Gehrcke plate and the telescope to observe the different polarizations of the observed light rays.

With a height adjustment of the telescope, one can move a crosshair in the ocular over the interference pattern. The position a of the crosshair is shown by a dial gauge.

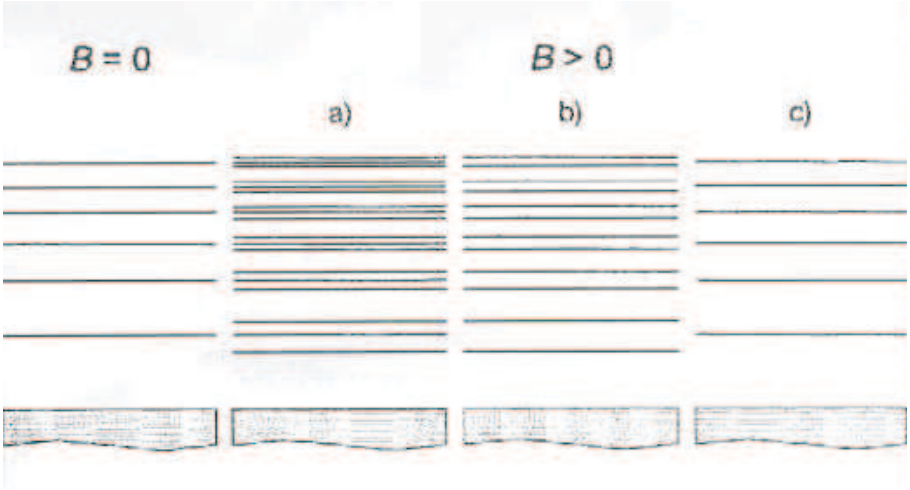

Figure 6: Interference pattern for the Zeeman effect observed in the transverse configuration a) without polarization filter, b) with polarization direction of the filter perpendicular to the magnetic field and c) with polarization direction of the filter parallel to the magnetic field.

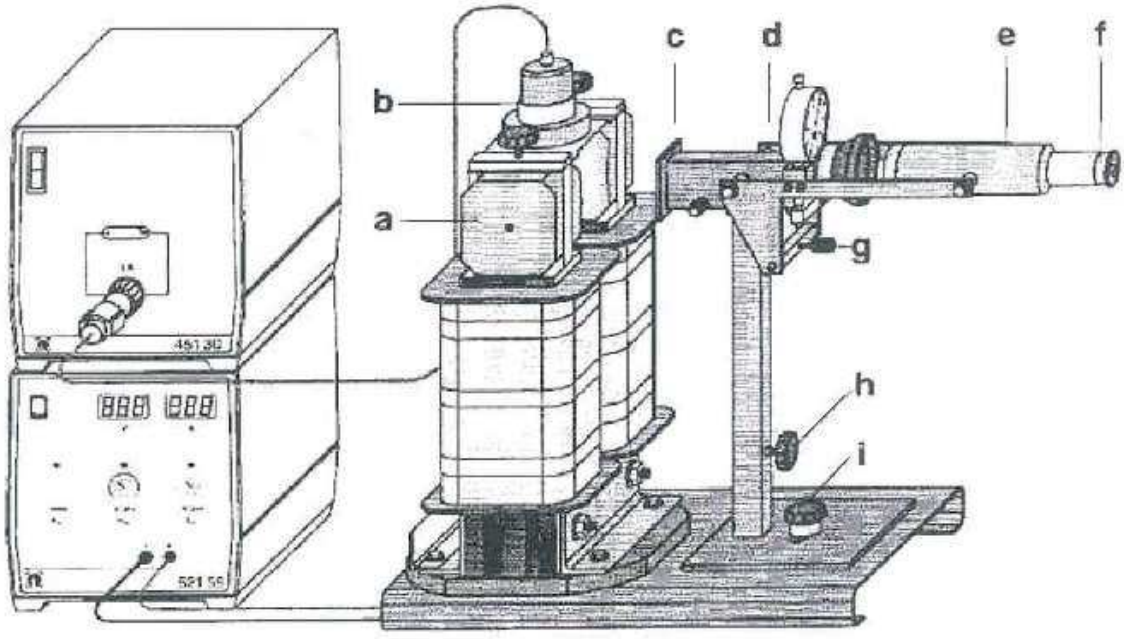

Figure 7: Sketch of the setup for studying the normal Zeeman effect (figure from Leybold, *Physics Leaflets*). a) magnet pole pieces, b) Cd-lamp, c) red filter, d) Lummer-Gehrcke-plate housing, e) telescope, f) ocular, g) height adjustment for telescope, h) arresting screw for column, i) arresting screw for column base

Part I: Objectives

- Use the Hall probe teslameter and measure the magnetic field strength at the position where the Cd lamp will be placed in dependence of the *Voltage* of the magnet power supply. Use steps of 1 Volts and measure both increasing and decreasing voltages (magnet hysteresis).
- Place the Cd lamp in the holder (avoid using any force!) and observe the Zeeman effect in both transversal and longitudinal direction.
- Use the polarizer and $\lambda/4$ plate and confirm the different light polarizations depending on the observation direction.
- In transversal observation direction, determine the positions a of all σ- and π-lines for $12-15$ interference orders at the voltages $U = 6\,\mathrm{V}$, $U = 9\,\mathrm{V}$, and $U = 12\,\mathrm{V}$.
- Data analysis: With help of table 2, correct the measured magnetic field strength values. Plot the corrected values of B versus the voltage, apply a linear fit. Use the fit result to determine the B-field strength at $U = 6\,\mathrm{V}$, $U = 9\,\mathrm{V}$, and $U = 12\,\mathrm{V}$.
- Data analysis: for each magnetic field, plot the interference order k versus the position a of the π-lines and find a polynomic function $k = f(a)$ that fits the data. The spacing of the different orders on the y-axis is $f(\Delta a) = f(a_2) - f(a_1) = 1$. Determine the ratios $\delta a/\Delta a$ with the fitted curve, calculate $\delta\lambda$ with Eq. 24 (Lummer-Gehrcke plate data: Refractive index $n = 1.4567$; thickness $d = 4.04\,\mathrm{mm}$).
- Data analysis: Calculate μ_B for the three magnetic field strengths and compare with the literature value of $\mu_B = 9.27400949 \cdot 10^{-24}\,\mathrm{J/T}$.

Safety notes:

- Do not remove the cover of the Lummer-Gehrcke plate, it's very expensive!
- When the magnet current is switched on, do not handle ferromagnetic objects in the vicinity of the cadmium lamp.
- Never touch the Cd lamp with your bare hands. Any moisture/fat can lead to friction forces in the lamp's glass that may break it when it's turned on, and it becomes very hot.

Table 2: Teslameter correction table

Increasing Voltage		Decreasing Voltage	
B measured	B accurate	B measured	corrected B
0.006	0.004	0.965	0.885
0.079	0.075	0.876	0.866
0.159	0.155	0.893	0.826
0.225	0.223	0.840	0.786
0.304	0.291	0.801	0.745
0.382	0.362	0.740	0.682
0.444	0.425	0.689	0.624
0.518	0.495	0.617	0.571
0.568	0.557	0.542	0.507
0.666	0.637	0.485	0.446
0.722	0.688	0.422	0.390
0.803	0.723	0.335	0.326
0.848	0.766	0.280	0.252
0.889	0.807	0.218	0.199
0.907	0.867	0.140	0.130
0.942	0.870	0.074	0.066
0.965	0.885	0.006	0.004

Part II: Precision spectroscopy

While the Lummer-Gehrcke plate used in the first part of the experiment is highly suited for measuring small wavelength differences, it cannot be used for wavelength determination. As you will learn in the second part of the experiment, one can perform highly accurate wavelength measurements using a grating spectrometer.

Czerny-Turner spectrometer

The Czerny-Turner (CT) spectrometer disperses light into discrete wavelengths by means of a grating. The spectral image is viewed in the exit focal plane using a two-dimensional CCD camera. A concave optical mirror (MC) is used to collimate the radiation entering the spectrometer through an entrance slit. After diffraction by the grating, the light is subsequently focused by a second concave mirror (MF) onto the CCD camera, as shown in Fig. 8.

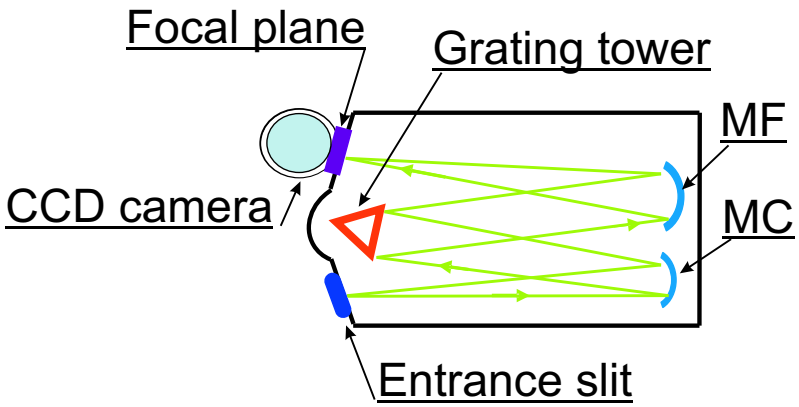

Figure 8: Illustration of the Czerny-Turner spectrometer.

Grating properties

In a grating, the incident and reflection angles of a light beam with a wavelength λ (see Fig. 9) are related by the following equation:

$$sin\alpha + sin\beta_k = kn\lambda \quad , \tag{25}$$

where α is the incidence angle, β_k is the diffraction angle relative to the grating normal (N_G), k is the diffraction order and n is the groove density ($1/d$). When $k = 0$, Eq. (25) is reduced to $\alpha = \beta_0$, the specular reflection law. If the diffraction

angle is fixed, the difference between α and β_k, the so-called deviation angle (D_V), is constant (see Fig. 9).

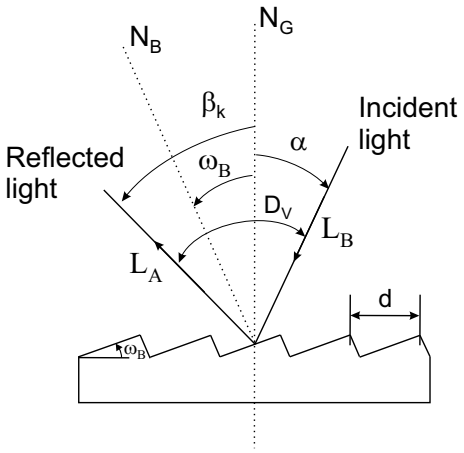

Figure 9: Scheme of the light reflexion in a grating. N_B is the blaze normal and ω_B defines the blaze angle. The distance between two consecutive grooves is defined by d.

A reflection grating can concentrate most of the diffracted spectral radiation into a single spectral order and, therefore, reduce the intensity of all other orders. This redistribution of intensity among the orders depends on the angle between the reflecting elements and the grating surface, which is called the *blaze angle* ω_B (see Fig. 9). In the visible spectrum, red light is deviated the least and violet the most.

Dispersion

The derivative of the diffraction angle over the wavelength is known as the *angular dispersion*. It is a measure of the angular separation between beams of adjacent wavelengths. An expression for the angular dispersion is derived by differentiating Eq. (25) for a fixed incident angle α:

$$\frac{\partial \beta_k}{\partial \lambda} = \frac{kn}{cos\beta_k} \quad . \tag{26}$$

High dispersion can be achieved either by choosing a grating with a high groove density (n), or by using a coarse grating in high diffraction order (k). The linear wavelength dispersion at the exit focal plane of a spectroscopic instrument is usually specified as *reciprocal linear dispersion* given in nm/mm. If the focal length of the instrument is L_B, then the reciprocal linear dispersion is given by:

$$D(\lambda) = \frac{\partial \lambda}{\partial p} = \frac{kncos\beta_k}{L_B} \quad , \tag{27}$$

where p represents the distance in mm. Since the size of the instrument depends on the focal length of the optical system, by choosing a grating with a high groove density, the instrument can be made more compact.

As shown in Eq. (27), the relation between the pixel position p on the CCD camera and the real wavelength λ is given by the dispersion function $D(\lambda)$. This function depends on the wavelength. At least one reference point p_0 in the spectrum (a known wavelenght λ_0) is required to calibrate the wavelength scale, if $D(\lambda)$ is known. Then the λ of any other line on the spectrum can be obtain by

$$\lambda = \lambda_0 + \int_{p_0}^{p} D(\lambda) dp \ . \tag{28}$$

This is, in general, difficult and often only numerically solveable because the dependence of the dispersion on the wavelength is trivial. If the dispersion function is independent of λ, Eq. (28) is expressed as

$$\lambda = \lambda_0 + D(p - p_0) \ , \tag{29}$$

and the desired wavelength λ can be determined.

In this experiment, you will use reference lines to find the dispersion function of the spectrometer. You can approximate the dispersion with the positions of the reference lines on the detector p_i and their respective wavelengths λ_i with a polynomial function $\lambda(p)$

$$\lambda(p) = A + B \cdot p + C \cdot p^2 + \dots \ , \tag{30}$$

where $A, B, C...$ are free parameters.

Resolution

The *resolution* or *chromatic resolving power* of a grating describes its ability to separate adjacent spectral lines. The resolution is generally defined as $\mathrm{R} = \frac{\lambda}{\Delta\lambda}$, where $\Delta\lambda$ is the difference in wavelength between two spectral lines with equal intensity that are separable.

The limit of resolution of a grating is $\mathrm{R} = k\mathrm{N}$, where N is the total number of grooves illuminated on the grating. A more practical expression for the resolution is obtained using Eq. (25)

$$R = kN = \frac{Nd(sin\alpha + sin\beta_k)}{\lambda} \ . \tag{31}$$

The spectrometer is equipped with a grating with 1800 groves/mm.

CCD detector

A CCD camera is a solid state detector array made of silicon with a sensitive range from 400 to 1100 nm. It converts the incoming light into electrons through the photoelectric effect. These free electrons are stored in a rectangular array of imaging elements called pixels defined by a grid of gate electrodes in the X and Y directions, respectively. The CCD provides simultaneously information for both intensities and positions projected along the height of the spectrograph image plane. The CCD chip size used is 30 × 12 mm^2 and is composed of 2048 × 512 pixels. Each pixel has an area of 15 × 15 μm^2. The camera is cooled with liquid nitrogen (LN2) to reduce thermal noise, and can integrate weak signals for hours without accumulating disturbing background (less than 1 electron/pixel/hour). The typical readout noise is less than 3 electrons/pixel at -140° C.

Calibration

Calibration lamp

In order to calibrate the spectrometer, i.e., to find the dispersion, reference lines are needed. For this purpose a neon calibration lamp is used. The used references lines, listed in Table 3, are taken from the spectral line database at NIST (National Institute for Standards and Technology, http://www.nist.gov/).

Table 3: Reference lines used for the calibration taken from *http://www.nist.gov/*

Species	***λ (nm)***	***Species***	***λ (nm)***	***Species***	***λ (nm)***
Ne I	585.24878	Ne I	621.72812	Ne I	667.82766
Ne I	588.18950	Ne I	626.64952	Ne I	671.70430
Ne I	594.48340	Ne I	630.47893	Ne I	692.94672
Ne I	597.55343	Ne I	633.44276	Ne I	702.40500
Ne I	602.99968	Ne I	638.29914	Ne I	703.24128
Ne I	607.43376	Ne I	640.22480	Ne I	717.39380
Ne I	609.61630	Ne I	650.65277	Ne I	724.51665
Ne I	614.30627	Ne I	653.28824	Ne I	743.88981
Ne I	616.35937	Ne I	659.89528		

Part II: Objectives

The aim of this experiment is to measure the wavelength of the red spectral line of Cd. Futhermore, another (very weak) line is emitted by the Cd lamp at $\approx 652\,\text{nm}$ wavelength. Using high precision wavelength determination, identify the element emitting this line.

- Preparation: The bandwith observed on the detector is $\approx 20\,\text{nm}$. Consequently, the grating has to be moved in order to project different parts of the Ne and Cd spectra on the CCD detector. The grating in the spectrometer converts wavelength/energy into a geometrical property, namely the dispersion on the CCD detector. As a result, one has to be careful about the geometry of the complete experimental setup (not only the spectrometer!) along the light path. Think about possible error sources in the measurement and how to circumvent them.

- Preparation: What is the expected shape of the spectral lines?

- Experiment: Take an overview spectrum of the light emitted by the Ne lamp showing all Ne lines listed in table 3. The spectrometer calibration is set to be off by more than 10 nm. Identify the Ne lines with the help of the reference spectrum lying out at the practicum.

- Experiment: Take an overview spectrum of the light emitted by the Cd lamp showing all four strong visible Cd lines.

- Experiment: Think of an optimal measurement strategy to minimize systematic errors (i.e. exposure time, calibration procedure, etc.). Discuss with the experiment supervisor before proceeding with the experiment.

- Experiment: Obtain calibration spectra and the necessary spectra of the Cd lamp for the high-precision measurements as discussed with the supervisor.

- Data Analysis: Determine wavelengths of the two red spectral lines emitted by the Cd lamp with the help of the Ne calibration lines and Eq. 30. Identify the unknown element with the help of the NIST Atomic Spectra Database (http://physics.nist.gov/PhysRefData/ASD/lines_form.html)

Appendix: Spectrometer control program

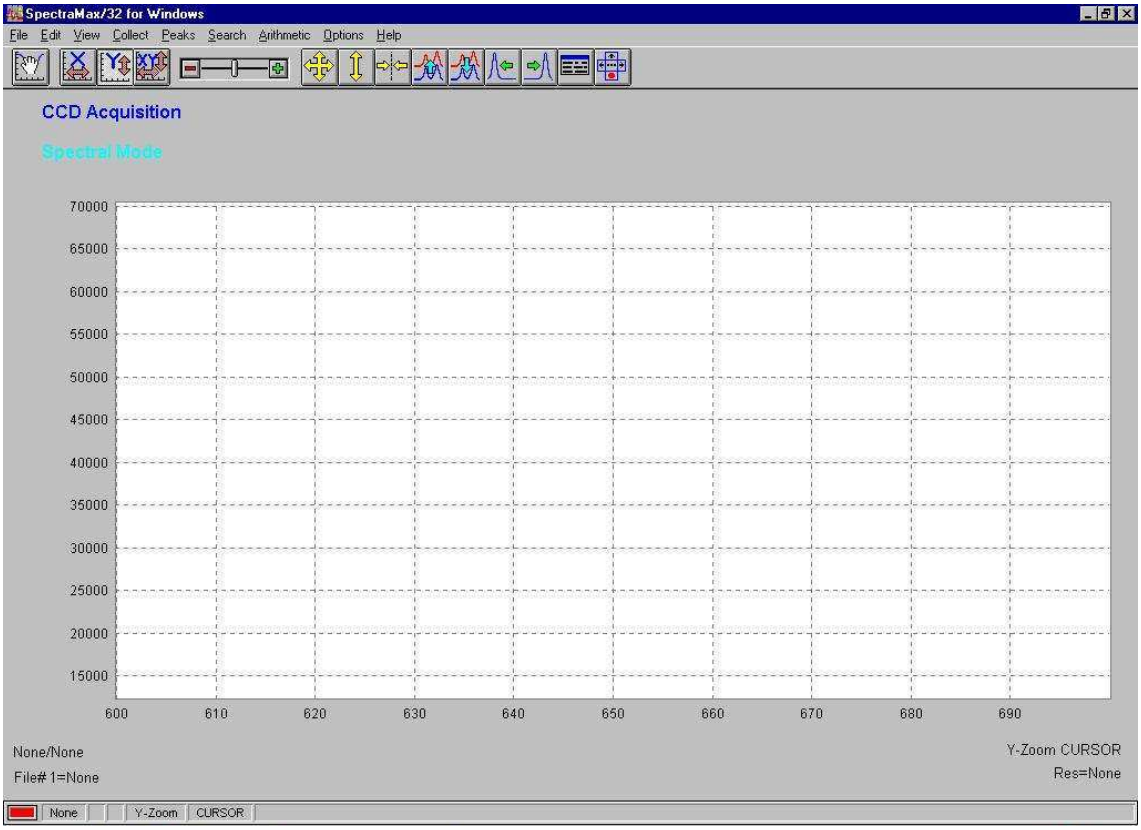

Figure 10: Main window of the spectrometer control program SPECTRAMAX by the company Jobin Yvon. You can zoom into spectra shown in the central part of the window by clicking and holding the left mouse button and dragging the mouse, and then left-clicking on the rectangle you created this way. You can return to viewing the full spectrum by clicking the button with the two perpendicular arrows in the top button row. By clicking the button showing a list (second from the right in the button row) you open the spectrometer control dialog shown in Fig. 11 on the next page

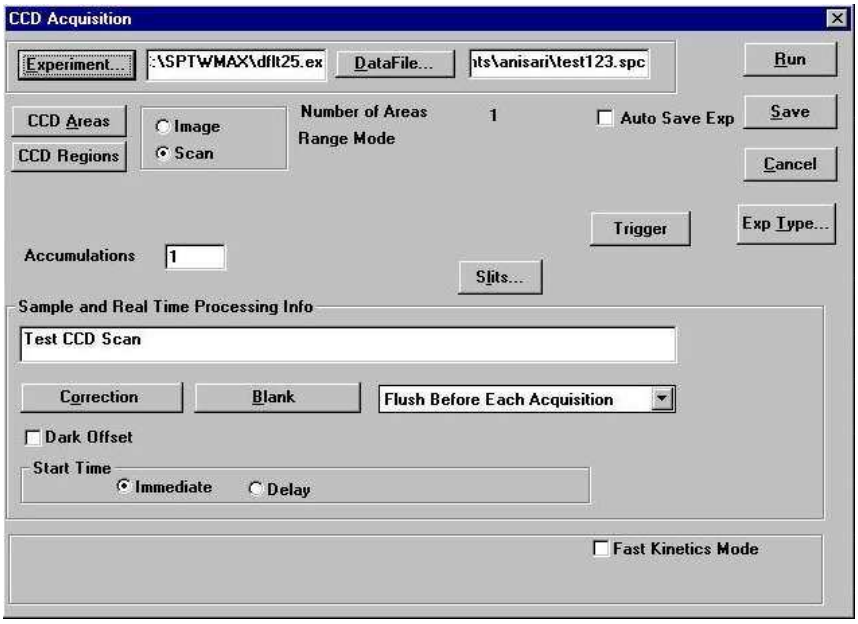

Figure 11: Spectrometer control dialog. Choose the name of a data file before taking a spectrum by clicking the button labelled 'Run'. CAUTION: do not use filenames with more than 8 characters! The button 'CCD Areas' opens the dialog shown in Fig. 12. The button 'CCD regions' opens the dialog shown in Fig. 13 and Fig. 14. The button 'Slits' opens the dialog shown in Fig. 15. All other controls are not needed for the experiment to be conducted.

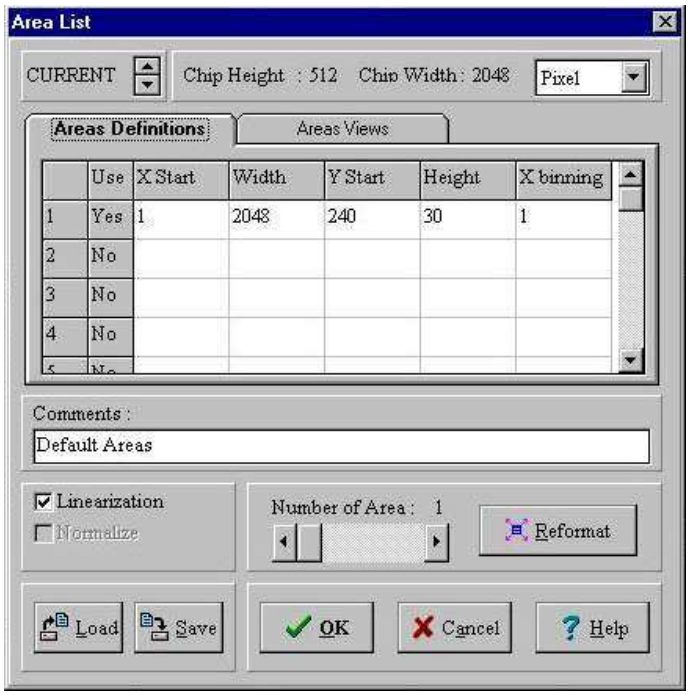

Figure 12: CCD areas dialog. Here you can define which CCD pixels you want to read out. The checkbox 'linearization' defines whether a spectrum is shown with a wavelength scale (linearization on) or pixel scale (linearization off).

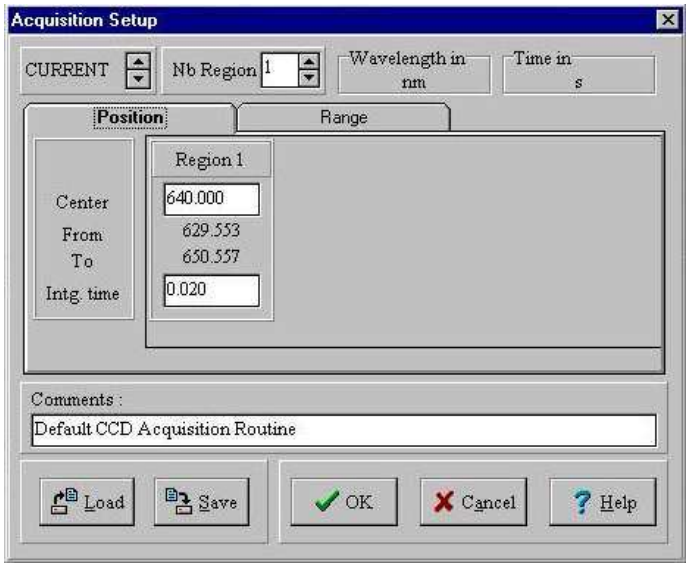

Figure 13: CCD regions dialog, Position tab. Here you can define which wavelength you want to project to the center of the CCD camera and the exposure time (integration time, in seconds). The spectrometer will move the grating once the button 'Run' is clicked in the spectrometer control dialog shown in Fig. 11.

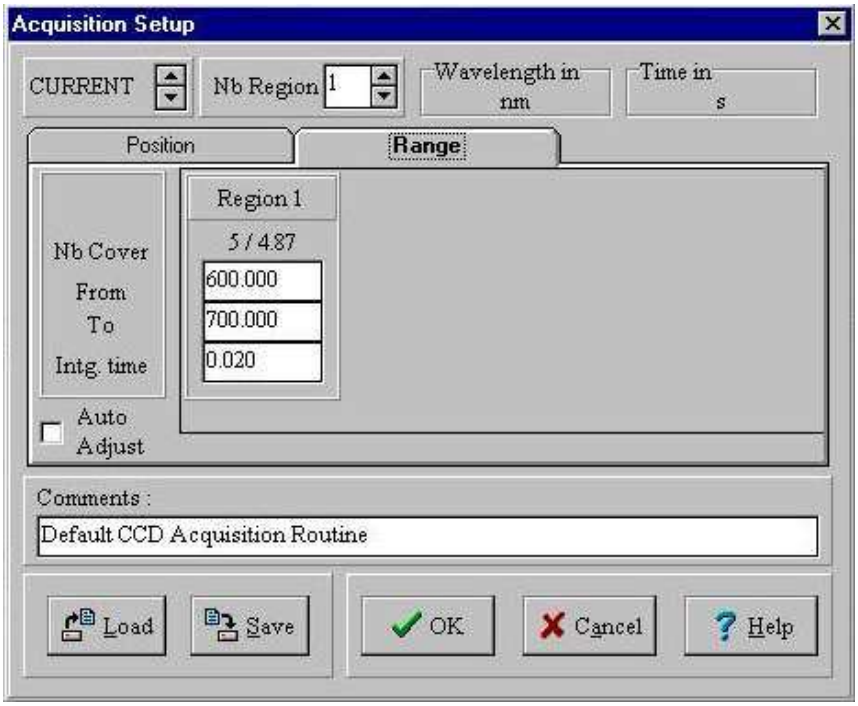

Figure 14: CCD regions dialog, Range tab. If you want to take an overview spectrum which is broader than the bandwidth covered in one position of the grating, use this dialog to define the lower and upper wavelength and the exposure time. The spectrometer will obtain a number of spectra (shown above the bandwidth selection as <exposures that will be made> / <exposures needed to cover selected bandwidth>) and automatically merge them afterwards once the button 'Run' is clicked in the spectrometer control dialog shown in Fig. 11.

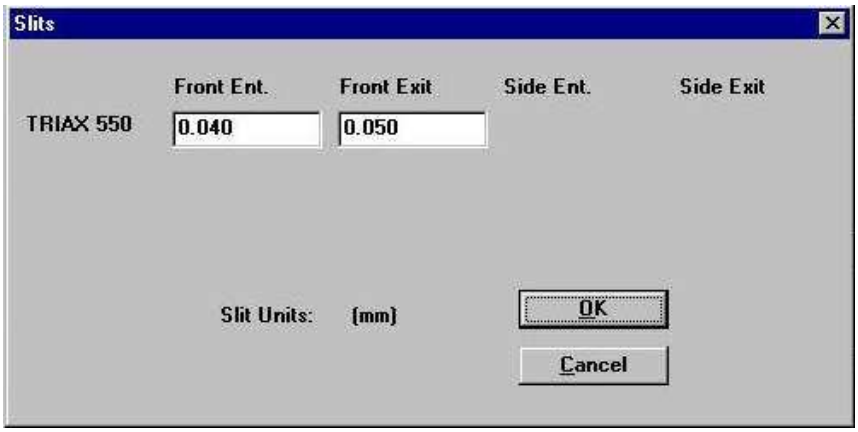

Figure 15: Slits dialog. The spectrometer is equipped only with an entrance slit. Here you can define the width of this slit (in mm). Note that depending on the intensity profile illuminating the entrance slit, changing the slit width during the experiment can lead to systematic errors.